THREE-PION DECAY $V \to \pi^+\pi^-\pi^0$ AND $V \to \pi^0\gamma^*$ TRANSITION FORM FACTORS ($V = \omega, \phi, J/\psi$) WITH KHURI–TREIMAN EQUATIONS*

Sergi González-Solís

Departament de Física Quàntica i Astrofísica, Universitat de Barcelona
Martí i Franquès, 1, 08028 Barcelona, Spain
and
Institut de Ciències del Cosmos, Universitat de Barcelona
Martí i Franquès, 1, 08028 Barcelona, Spain

Received 7 May 2026, accepted 23 June 2026, published online 10 July 2026

We study the three-pion decays of vector mesons, $V \to \pi^+\pi^-\pi^0$ ($V = \omega, \phi, J/\psi$), within the framework of Khuri–Treiman to account for analyticity, unitarity, and crossing symmetry. Using once-subtracted dispersion relations, we perform a simultaneous analysis of the $\omega, \phi \to 3\pi$ Dalitz plot and of the $\omega/\phi \to \pi^0\gamma^*$ transition form factor measurements finding good agreement with these experimental data. We also analyze the di-pion invariant mass distributions of the vector charmonium decay $J/\psi \to 3\pi$ experimental data, and predict the $J/\psi \to \pi^0\gamma^*$ form factor.

DOI:10.5506/APhysPolBSupp.19.4-A10

1. Introduction

In this work, we review the dispersive analyses of the three-pion decay modes of vector mesons, $V \to \pi^+\pi^-\pi^0$ ($V = \omega, \phi, J/\psi$), and of the transition form factors, $V \to \pi^0\gamma^*$, carried out by the JPAC Collaboration in Refs. [3, 6, 10].

2. Formalism

2.1. Decay amplitude and kinematics

The $V(p_V) \to \pi^0(p_0)\pi^+(p_+)\pi^-(p_-)$ amplitude can be expressed as

$$\mathcal{M}(s,t,u) = i\,\epsilon_{\mu\nu\alpha\beta}\,\epsilon^{\mu}(p_V)\,p_+^{\nu}\,p_-^{\alpha}\,p_0^{\beta}\,F(s,t,u)\,, \tag{1}$$

* Presented at the Excited QCD 2026 Workshop, Granada, Spain, 8–14 January, 2026.

where $\epsilon_{\mu\nu\alpha\beta}$ is the Levi-Civita tensor, $\epsilon^{\mu}(p_V)$ is the polarization vector of the decaying V meson, and $F(s,t,u)$ is the single invariant scalar function containing the dynamical information. The particle momenta are related to the Mandelstam variables through: $s = (p_+ + p_-)^2$, $t = (p_0 + p_+)^2$, $u = (p_0 + p_-)^2$ with $s + t + u = m_V^2 + 3m_\pi^2$ (in the isospin limit with $m_\pi = m_{\pi^\pm}$).

The scattering angle in the s-channel, defined by the center of mass of the $\pi^+\pi^-$ pair, is denoted by θ_s and is given by $\cos\theta_s(s,t,u) = (t-u)/(4\,p(s)\,q(s))$ and $\sin\theta_s(s,t,u) = (\sqrt{\phi(s,t,u)})/(2\sqrt{s}\,p(s)\,q(s))$, where $p(s) = \lambda^{1/2}(s,m_\pi^2,m_\pi^2)/(2\sqrt{s}\,)$ and $q(s) = \lambda^{1/2}(s,m_V^2,m_\pi^2)/(2\sqrt{s}\,)$ are, respectively, the momenta of the $\pi^\pm$ and π^0 in the s-channel, and where $\lambda(a,b,c) = a^2 + b^2 + c^2 - 2ab - 2bc - 2ca$ is the Källén, or triangle, function. The zeroes of the Kibble function, $\phi(s,t,u) = (2\sqrt{s}\,\sin\theta_s\,p(s)\,q(s))^2 = s\,t\,u - m_\pi^2(m_V^2 - m_\pi^2)^2$, define the boundaries of the physical regions of the process. The Dalitz-plot boundaries in t for a given value of s for $V \to 3\pi$ lie within the interval $[t_{\min}(s),\ t_{\max}(s)]$, with $t_{\max,\min}(s) = \frac{m_V^2+3m_\pi^2-s}{2} \pm 2\,p(s)\,q(s)$, while the allowed range for s is given by $s_{\min} = 4m_\pi^2$ to $s_{\max} = (m_V - m_\pi)^2$. Finally, the differential decay width reads

$$\frac{\mathrm{d}^2\Gamma}{\mathrm{d}s\,\mathrm{d}t} = \frac{1}{(2\pi)^3}\,\frac{1}{32\,m_V^3}\,\frac{1}{3}\frac{\phi(s,t,u)}{4}\,|F(s,t,u)|^2\,. \tag{2}$$

2.2. Khuri–Treiman equations for $V \to \pi^+\pi^-\pi^0$ ($V = \omega, \phi, J/\psi$)

The Khuri–Treiman (KT) formalism for the $V \to 3\pi$ amplitude $F(s,t,u)$ is well-established [1–6]. As shown in these references, the s-channel partial-wave expansion for $F(s,t,u)$ is given by

$$F(s,t,u) = \sum_{J\,\mathrm{odd}}^{\infty} (p(s)\,q(s))^{J-1}\,P'_J(z_s)\,f_J(s)\,, \tag{3}$$

where $z_s = \cos\theta_s$, $P'_J(z_s)$ is the Legendre polynomial derivative, and $f_J(s)$ is the partial waves of total angular momentum J. The KT representation of $F(s,t,u)$ in Eq. (3) is obtained by replacing the infinite sum of partial waves in the s-channel with the sum of three so-called isobar amplitudes, one for each of the s-, t-, and u-channels. Truncating the partial-wave expansion of each isobar amplitude at $J_{\max} = 1$, we obtain the following crossing-symmetric isobar decomposition [1–3, 6]: $F(s,t,u) = F_1(s) + F_1(t) + F_1(u)$, where each isobar amplitude, $F_1(x)$, has only a right-hand or unitary cut in its respective Mandelstam variable. The relation between $F_1(s)$ and $f_1(s)$ is obtained by projecting $F(s,t,u)$ onto the s-channel partial wave

$$f_1(s) = F_1(s) + \hat{F}_1(s)\,, \qquad \hat{F}_1(s) \equiv 3 \int\limits_{-1}^{1} \frac{\mathrm{d}z_s}{2} \left(1 - z_s^2\right)\, F_1(t(s, z_s))\,, \tag{4}$$

where the inhomogeneity $\hat{F}_1(s)$ contains the s-channel projection of the left-hand cut contributions due to the t- and u-channels, and its evaluation in the decay region requires a proper analytical continuation [8]. Assuming elastic unitarity with only two-pion intermediate states, we arrive at the KT equation for the $V \to 3\pi$ decay, *i.e.* the unitarity relation for the isobar amplitude $F_1(s)$: $\mathrm{disc}\, F_1(s) = 2i(F_1(s) + \hat{F}_1(s)) \sin\delta_1(s)\, \mathrm{e}^{-i\delta_1(s)}\theta(s - 4m_\pi^2)$, where $\delta_1(s)$ is the P-wave $\pi\pi$ phase shift, which is real.

Given the discontinuity relation above, one can write an unsubtracted dispersion relation for $F_1(s)$ as

$$F_1(s) = \frac{1}{2\pi i} \int\limits_{4m_\pi^2}^{\infty} \mathrm{d}s'\, \frac{\mathrm{disc}\, F_1(s')}{s' - s}\,, \tag{5}$$

the solution of which can be written as

$$F_1(s) = \Omega_1(s) \left(a + \frac{s}{\pi} \int\limits_{4m_\pi^2}^{\infty} \frac{\mathrm{d}s'}{s'}\, \frac{\sin\delta_1(s')\, \hat{F}_1(s')}{|\Omega_1(s')|\,(s' - s)} \right)\,, \tag{6}$$

where $\Omega_1(s)$ is the usual Omnès function [9]

$$\Omega_1(s) = \exp\left[\frac{s}{\pi} \int\limits_{4m_\pi^2}^{\infty} \frac{\mathrm{d}s'}{s'}\, \frac{\delta_1(s')}{s' - s} \right]\,. \tag{7}$$

The subtraction constant a in Eq. (6) is the only free parameter in the model. It is in general complex, $a = |a|\, \mathrm{e}^{i\phi_a}$, and can be factored out ($\hat{F}_1(s)$ shares phase with a through Eq. (4)) since it determines the overall normalization of the amplitude. While its modulus $|a|$ can be fixed from the experimental $V \to 3\pi$ decay width, no observable of the decay is sensitive to the overall phase ϕ_a, so we can set $\phi_a = 0$.

One can write a once-subtracted dispersion relation for $F(s)$ in the form

$$F_1(s) = \Omega_1(s) \left(a + b'\, s + \frac{s^2}{\pi} \int\limits_{4m_\pi^2}^{\infty} \frac{\mathrm{d}s'}{(s')^2}\, \frac{\sin\delta_1(s')\, \hat{F}_1(s')}{|\Omega_1(s')|\,(s' - s)} \right)\,, \tag{8}$$

where b' satisfies the following sum rule [1]:

$$b \equiv b'/a = \frac{1}{\pi} \int\limits_{4m_\pi^2}^{\infty} \frac{\mathrm{d}s'}{(s')^2} \, \frac{\sin\delta_1(s')\,\hat{F}_1(s')/a}{|\Omega_1(s')|} \,. \tag{9}$$

Performing one subtraction on Eq. (5) leads to the solution [1, 3, 6]: $F_1(s) = a[F_a(s) + b\,F_b(s)]$, where now b is not constrained to satisfy Eq. (9), and the functions $F_a(s)$ and $F_b(s)$ are given by

$$F_a(s) \;=\; \Omega_1(s) \left[1 + \frac{s^2}{\pi} \int\limits_{4m_\pi^2}^{\infty} \frac{\mathrm{d}s'}{s'^2} \, \frac{\sin\delta_1(s')\,\hat{F}_a(s')}{|\Omega_1(s')|(s'-s)} \right] , \tag{10}$$

$$F_b(s) \;=\; \Omega_1(s) \left[s + \frac{s^2}{\pi} \int\limits_{4m_\pi^2}^{\infty} \frac{\mathrm{d}s'}{s'^2} \, \frac{\sin\delta_1(s')\,\hat{F}_b(s')}{|\Omega_1(s')|(s'-s)} \right] . \tag{11}$$

These functions only need to be calculated once since they are independent of the numerical values of the fit parameters a and b. As a matter of example, in Fig. 1, we show the solutions for the $\phi \to 3\pi$ decay for $F_a(s)$ using a numerical iterative procedure detailed in Refs. [3, 6, 10].

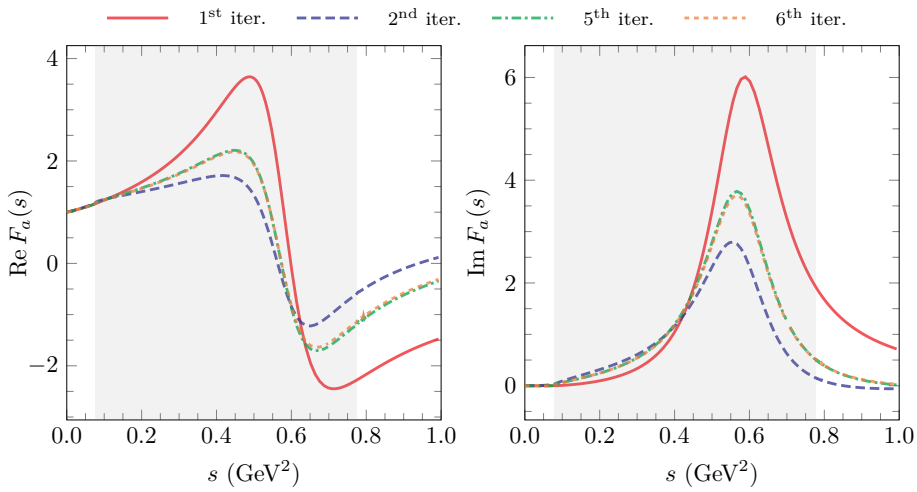

Fig. 1. Convergence behavior of the iterative procedure for the real (left plot) and imaginary (right plot) parts of the amplitudes $F_a(s)$ (Eq. (10)). The shaded area represents the physical $\phi \to 3\pi$ decay region, *i.e.*, $4m_\pi^2 \ll s \ll (m_\phi - m_\pi)^2$.

2.3. Transition form factor $V \to \pi^0\gamma^*$

We introduce here the $V \to \pi^0\gamma^*$ transition form factor $f_{V\pi^*}(s)$. We include the two-pion intermediate state contribution to the discontinuity

$$\mathrm{disc} f_{V\pi^0}(s) = i\,\frac{p^3(s)}{6\pi\sqrt{s}}\,F_\pi^{V\,*}(s)\,f_1(s)\,\theta\left(s-4m_\pi^2\right)\,, \tag{12}$$

which requires as input the $V \to 3\pi$ amplitude $f_1(s)$ given in Eq. (4) and the pion vector form factor complex-conjugate $F_\pi^{V\,*}(s)$, which we approximate by the Omnès function (complex-conjugate) given in Eq. (7). We use a once-subtracted dispersion relation for the TFF of the form

$$f_{V\pi^0}(s) = |f_{V\pi^0}(0)|\,\mathrm{e}^{i\phi_{V\pi^0}(0)} + \frac{s}{12\pi^2}\int\limits_{4m_\pi^2}^{\infty}\frac{\mathrm{d}s'}{(s')^{3/2}}\,\frac{p^3(s')\,F_\pi^{V\,*}(s')\,f_1(s')}{(s'-s)}\,. \tag{13}$$

The modulus of the subtraction constant $|f_{V\pi^0}(0)|$ can be fixed from the measured $V \to \pi^0\gamma$ partial decay width

$$\Gamma\left(V\to\pi^0\gamma\right) = \frac{e^2\left(m_V^2-m_{\pi^0}^2\right)^3}{96\pi m_V^3}\,|f_{V\pi^0}(0)|^2\,, \tag{14}$$

while the phase $\phi_{V\pi^0}(0)$ is a free parameter that can only be accessed from the transition form factor experimental data (see *e.g.* Ref. [3]).

3. Results

We compare our KT amplitudes defined in the previous section to the following experimental information: *(i)* the $\omega \to 3\pi$ Dalitz-plot parameters from BESIII [11] and $\omega \to \pi^0\gamma^*$ TFF experimental data by the A2 [12] and NA60 [13] collaborations; *(ii)* the measurement of the $\phi \to 3\pi$ decay Dalitz plot [14] and the transition form factor $\phi \to \pi^0\gamma^*$ [15] by KLOE; *(iii)* the di-pion mass projection of the $J/\psi \to 3\pi$ experimental data from BESIII [16]. In the following, we highlight the main findings from Refs. [3, 6, 10].

For $\omega \to 3\pi$, we find good agreement between the BESIII Dalitz-plot parameters and our results, as it can be seen in Table 1. In Fig. 2, we present the residuals for the $\phi \to 3\pi$ Dalitz plot, defined as the difference for each bin between the theoretical fitted and experimental values from KLOE divided by the experimental error. As we observe, the residuals do not show any patterns, suggesting that no regions in the Dalitz plot are described better than others. Furthermore, we have verified that the distribution of residuals approximately follows a normal distribution centered around zero, with a standard deviation of one. In summary, all of these observations,

combined with the values of $\chi^2/\text{d.o.f.} \simeq 1$, confirm that the description of the event distribution throughout the Dalitz-plot region is very accurate. Lastly, the result of the fit to the $J/\psi \to 3\pi$ experimental data from BESIII is shown in Fig. 2. It can be seen that the fit provides a satisfactory description of the $\rho(770)$ shape seen in the data.

Table 1. BESIII $\omega \to 3\pi$ [11] Dalitz-plot parameters α, β, γ, and our results from [3].

Dalitz parameters	$\alpha \times 10^3$	$\beta \times 10^3$	$\gamma \times 10^3$
BESIII	111(18)	25(10)	22(29)
This work I	112(15)(2)	23(6)(2)	29(6)(8)
This work II	109(14)(2)	26(6)(2)	19(5)(4)

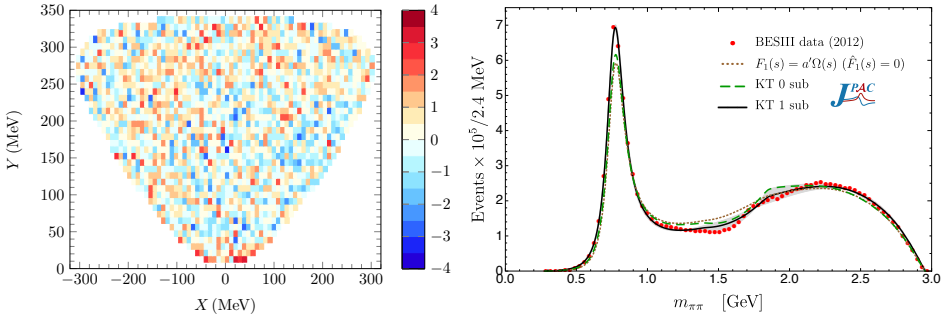

Fig. 2. (Color online) Left: Residuals for the $\phi \to 3\pi$ Dalitz plot (see the main text for details). Right: BESIII (red circles) [16] measurement of the $m_{\pi\pi}$ invariant mass distribution for $J/\psi \to 3\pi$ as compared to our fit (black solid line). See Refs. [6, 10] for details.

We now discuss the value of the subtraction constant b. We present the fitted value in the lower part of Table 2, while the upper part displays the value of the sum rule b_{sum} (*cf.* Eq. (9)). A comparison between the $\omega \to 3\pi$ and $\phi \to 3\pi$ cases reveals a striking difference in the value of the subtraction constant. In the ϕ case, the fitted value is close to the sum-rule value, which would reduce the once-subtracted dispersion relation to an unsubtracted form. This sharply contrasts with the ω case, where the fitted value significantly deviates from the sum rule. As discussed in Ref. [3], this deviation is primarily driven by the transition form factor high-energy data points from NA60. These intriguing difference should encourage new experimental analyses. The subtraction for the $J/\psi \to 3\pi$ stays close to its sum-rule prediction. Therefore, we conclude that the $\pi\pi$ P-wave phase shift saturates the sum rule for the $J/\psi \to 3\pi$ partial wave to about 75%.

Table 2. Values of the parameter b given by the sum rule (upper part) and obtained through the fit (lower part) for each process. See Ref. [3] for details.

Subtraction constant	ω	ϕ	J/ψ
b_{sum}	$0.55\,\mathrm{e}^{0.15\,i}$	$0.79\,\mathrm{e}^{0.69\,i}$	$0.141\,\mathrm{e}^{2.321\,i}$
b_{fit}	$2.65(35)\,\mathrm{e}^{1.70(27)\,i}$	$0.76\,\mathrm{e}^{0.43\,i}$	$0.198(35)\,\mathrm{e}^{2.675(300)\,i}$

Finally, the results for the $\omega \to \pi^0\gamma^*$ and $\phi \to \pi^0\gamma^*$ TFF are shown in Fig. 3 (see Ref. [6] for our predictions of $J/\psi \to \pi^0\gamma^*$). It can be seen that both of them agree well with the experimental data, except for the highest two points of the NA60 data for $\omega \to \pi^0\gamma^*$ and that our description for $\phi \to \pi^0\gamma^*$ falls slightly below the central values.

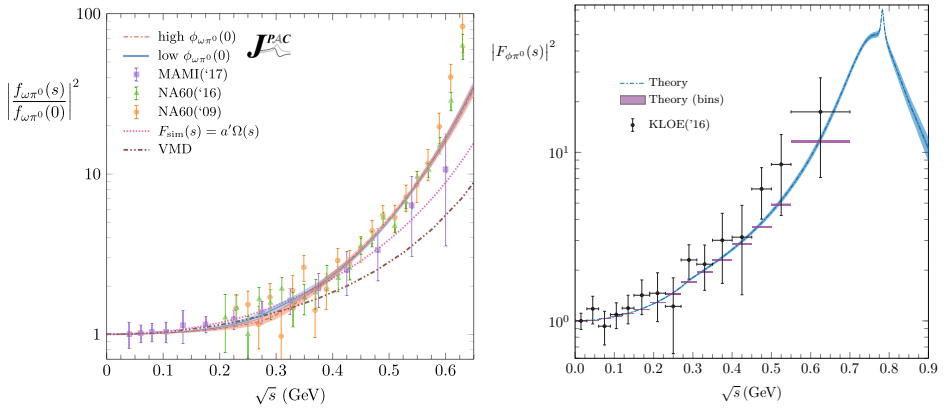

Fig. 3. Normalized transition form factor modulus squared in logarithmic scale as a function of $\sqrt{s}$ of the processes $\omega \to \pi^0\gamma^*$ (left) and $\phi \to \pi^0\gamma^*$ (right).

4. Summary

In this work, we have shown that the Khuri–Treiman equations provide a robust theoretical framework for the analyses of the $V \to 3\pi$ decays and $V \to \pi^0\gamma^*$ transition form factors incorporating the fundamental principles of analyticity, unitarity, and crossing symmetry via dispersion relations.

This work was supported by FEDER UE through grant PID2023-147112NB-C21, as well as through the award "Unit of Excellence María de Maeztu 2025–2029" to the Institute of Cosmos Sciences, grant CEX2024-001451-M funded by MICIU/AEI/10.13039/501100011033. Additional support was provided by the Generalitat de Catalunya (AGAUR) through grant 2021SGR01095. S.G-S. is the Serra Húnter Fellow.

REFERENCES

[1] F. Niecknig, B. Kubis, S.P. Schneider, *Eur. Phys. J. C* **72**, 2014 (2012).

[2] I.V. Danilkin *et al.*, *Phys. Rev. D* **91**, 094029 (2015).

[3] JPAC Collaboration (M. Albaladejo *et al.*), *Eur. Phys. J. C* **80**, 1107 (2020).

[4] JPAC Collaboration (M. Albaladejo *et al.*), *Prog. Part. Nucl. Phys.* **127**, 103981 (2022).

[5] B. Kubis, F. Niecknig, *Phys. Rev. D* **91**, 036004 (2015).

[6] JPAC Collaboration (M. Albaladejo *et al.*), *Phys. Rev. D* **108**, 014035 (2023).

[7] JPAC Collaboration (M. Albaladejo *et al.*), *Phys. Rev. D* **101**, 054018 (2020).

[8] J.B. Bronzan, C. Kacser, *Phys. Rev.* **132**, 2703 (1963).

[9] R. Omnès, *Nuovo Cim.* **8**, 316 (1958).

[10] JPAC Collaboration (A. Garcia-Lorenzo *et al.*), arXiv:2505.15309 [hep-ph].

[11] BESIII Collaboration (M. Ablikim *et al.*), *Phys. Rev. D* **98**, 112007 (2018).

[12] A2 Collaboration at MAMI (P. Adlarson *et al.*), *Phys. Rev. C* **95**, 035208 (2017).

[13] NA60 Collaboration (R. Arnaldi *et al.*), *Phys. Lett. B* **757**, 437 (2016).

[14] KLOE Collaboration (A. Aloisio *et al.*), *Phys. Lett. B* **561**, 55 (2003); *Erratum ibid.* **609**, 449 (2005).

[15] KLOE-2 Collaboration (A. Anastasi *et al.*), *Phys. Lett. B* **757**, 362 (2016).

[16] BESIII Collaboration (M. Ablikim *et al.*), *Phys. Lett. B* **710**, 594 (2012).